Microchimica Acta (2021) 188: 41
https://doi.org/10.1007/s00604-020-04692-y

ORIGINAL PAPER

Impedimetric determination of cortisol using screen-printed electrode with aptamer-modified magnetic beads

Pannaporn Pusomjit[1] · Prinjaporn Teengam[1] · Nichanan Thepsuparungsikul[2] · Sucharat Sanongkiet[2] · Orawon Chailapakul[1]

Received: 16 August 2020 / Accepted: 22 December 2020 / Published online: 15 January 2021

Abstract

A non-invasive aptamer-based electrochemical biosensor using disposable screen-printed graphene electrodes (SPGEs) was developed for simple, rapid, and sensitive determination of cortisol levels. Selective detection of cortisol based on a label-free electrochemical assay was achieved by specific recognition of the cortisol DNA aptamer (CApt). The CApt was modified with streptavidin magnetic beads (MBs) before simple immobilization onto the electrode surface using a neodymium magnet. The electrochemical behavior of the aptamer-based biosensor was assessed by using electrochemical impedance spectroscopy (EIS) and cyclic voltammetry (CV) (vs Ag/AgCl). The specific binding between cortisol and CApt resulted in a decrease in charge transfer resistance (R_{ct}) from EIS using $[Fe(CN)_6]^{3-/4-}$ with increasing cortisol concentration. Under optimal conditions, a linear range from 0.10 to 100 ng/mL with a low detection limit (3SD/slope) of 2.1 pg/mL was obtained. Furthermore, the proposed biosensing system exhibited a satisfactory recovery in the range 97.4–109.2% with 5.7–6.6% RSD in spiked artificial human sweat. Regarding the applications of this tool, the aptamer-based biosensor has potential to be a versatile and point-of-care (POC) device for simple, sensitive, selective, disposable, and low-cost cortisol detection.

Keywords Aptamer · Electrochemical impedance spectroscopy · Non-invasive · Cortisol · Label-free · Screen-printed graphene electrode

Introduction

Cortisol or hydrocortisone is one of the steroid hormones produced by the adrenal glands [1, 2]. Cortisol has been recognized as a "stress hormone" since its levels affect the psychological stress and relate to negative health outcomes. Moreover, long-term cortisol exposure in the human body can cause several adverse health effects such as heart attack, obesity, Cushing's syndrome, Addison's disease, depression disorder, and post-traumatic stress disorder (PTSD) [3]. Generally, high cortisol levels can be observed in the morning and the levels progressively decrease at night [2, 4, 5]. Cortisol is present in various measurable biological samples such as serum [6, 7], urine [8], saliva [3, 9], and sweat [5, 10]. Among these samples, sweat is extensively evaluated as a non-invasive bio-fluid, since it provides the medical information to detect free cortisol with a normal level in the range of 8–140 ng/mL [10]. Furthermore, it can be continuously and simply obtained from the surface area outside the human body without external contamination and because it contains a low concentration of proteins, peptides, amines, amino acids, and metal ions [11, 12].

Traditional cortisol diagnosis has been performed by various methods such as chromatographic methods coupled with mass spectrometry [8], enzyme-linked immunosorbent assay (ELISA) [13], chemiluminescence immunoassay [1], surface plasmon resonance (SPR) [6], and quartz crystal microbalance (QCM) [14]. Although all of these methods demonstrate high sensitivity, they have limitations because they rely on bulky, complicated, and expensive instruments and trained operators [2, 7], which limit their potential for point-of-care (POC)

✉ Nichanan Thepsuparungsikul
tepsuparungsiku_n@su.ac.th

✉ Orawon Chailapakul
corawon@chula.ac.th

[1] Electrochemistry and Optical Spectroscopy Center of Excellence (EOSCE), Department of Chemistry, Faculty of Science, Chulalongkorn University, Pathumwan, Bangkok 10330, Thailand

[2] Department of Chemistry, Faculty of Science, Silpakorn University, Amphoe Muang, Nakhon Pathom 73000, Thailand

applications. Electrochemical immunoassay provides a series of advantages including high sensitivity, small sample requirement, short time analysis, portable, and low cost [9, 15], which satisfy the requirements for point-of-care testing (POCT). To obtain a sensitive electrochemical signal, this method employs the labels or electroactive indicators, including redox couple such as metal ion complex [16], methylene blue [17], and anthraquinone [18]. Since a labelling procedure is involved, these strategies are limited by a time-consuming and complicated detection process. To overcome such limitations, a label-free immunoassay has been developed. The label-free system provides simple and rapid detection without requiring a labelling step and is detectable in terms of mechanical [19], optical [10], and electrical [20] signals. Electrochemical impedance spectroscopy (EIS) has proven to be an increasingly popular label-free technique for ultrasensitive diagnostic sensors [16, 21]. The EIS-based biosensor provides potential for developing point-of-care sensing device when combined with portable instrument due to its simple fabrication, the ability to separate surface binding events from the solution impedance, ease of signal quantification, and little damage to biological interactions during measurement [22, 23]. The most recognition system in terms of electrochemical immunoassay is established on the specific recognition between antigen and antibody. Although a good sensitivity was achieved, its limitations are that requires large molecules, in vivo generation, difficulty in chemical modification, and low stability at high temperature [24, 25]. Recently, the aptamer-based electrochemical biosensor for cortisol detection has been reported due to its high sensitivity, specificity, long-term stability, easy fabrication, and low cost [5, 7, 20]. Aptamers are small (usually 10–100 nucleotides) single-stranded oligonucleotide (DNA or RNA) with high affinity and specificity for target molecules such as metal ions, amino acids, antibiotics, vitamins, peptides, proteins, and microorganisms [26, 27]. Aptamers provide significant advantages over antibody, including ease of in vitro synthesis through systematic evolution of ligands by exponential enrichment (SELEX), ease of chemical modification, cost-effectiveness, and high stability [28, 29]. Thus, aptamers have attracted increasing attention for diagnostics and therapeutics.

Generally, direct attachment to gold and covalent attachment to functionally modified electrode surface are commonly used to immobilize aptamers for electrochemical biosensor. Nevertheless, time-consuming, complication step and reproducibility are major challenges of these methods [30, 31]. Streptavidin magnetic beads (MBs) have been utilized for immobilization of aptamers on electrode surface. This is due to the fact that MBs can minimize analysis time, simply immobilize onto the electrode surface by magnetic attachment, and reduce the matrix effect [20, 32]. In addition, aptamer-modified magnetic beads have been prepared in batch scale resulting in good reproducibility [33].

In this study, an aptamer-based electrochemical impedance biosensor was proposed for the non-invasive determination of free cortisol. Magnetic beads modified with cortisol DNA aptamers were simply immobilized onto the electrode surface using a neodymium magnet. Electrochemical impedance spectroscopy was used to determine the cortisol concentration by measuring the fractional change in the charge transfer resistance (R_{ct}) using the $[Fe(CN)_6]^{3-/4-}$ redox solution. A good linear relationship between the changes in charge-transfer resistance (ΔR_{ct}) and cortisol concentration was demonstrated. The proposed system was successfully applied with artificial human sweat. This aptamer-based sensing platform is promising as a simple, non-invasive, sensitive, and selective device for POC cortisol diagnosis.

Experimental

Chemicals and materials

All reagents were of analytical reagent grade, and all solutions were prepared using Milli-Q water from Millipore ($R \geq 18.2$ M Ω cm at 25 °C). Cortisol DNA aptamer (CApt) modified with biotin (5′-biotin-AGC AGC ACA GAG GTC AGA TGC AAA CCA CAC CTG AGT GGT TAG CGT ATG TCA TTT ACG GAC C-3′) (61 bp) [20] was purchased from IDT-DNA (Coralville, IA). Streptavidin magnetic beads (MBs) at 1 μm were sourced by New England Biolabs (Ipswich, MA). Hydrocortisone (cortisol) solution and urea were obtained from Sigma-Aldrich (St. Louis, USA). Cortisone and corticosterone were supplied by Glentham Life Sciences (Wiltshire, UK). Acetic acid was purchased from CARLO ERBA (Peypin, France). Lactic acid was obtained from BDH Prolabo (Karnataka, India). All standard solutions were prepared with a wash/binding buffer (0.5 mM NaCl (CARLO ERBA), 20 mM Tris-HCl (Sigma-Aldrich), 1 mM Ethylenediaminetetraacetic acid (EDTA)); pH 7.5 (Riedel-deHaën) and stored at − 20 °C until use. Artificial human sweat (86.89% H_2O, 7.62% NaOH, 1.9% NaCl, 1.67% NH_4Cl, 1.21% lactic acid, 0.48% urea and 0.24% acetic acid) was obtained from Moulage Sciences & Training (Illinois, USA).

Graphene and silver/silver chloride (Ag/AgCl) inks were purchased from Gwent Group (Torfaen, UK). The screen-printed pattern was designed using Adobe Illustrator and was made by Chaiyaboon Co. Ltd., (Bangkok, Thailand, http://www.chaiyaboon.com). The design of SPGE is shown in the previous work [34].

Fabrication of the screen-printed graphene electrode

For electrode fabrication, three electrode systems were prepared using an in-house screen-printing method according to

a previously reported protocol [18]. The design and screen-printed graphene electrode (SPGE) preparation steps are shown in Fig. S1, supplementary material. After SPGE preparation, the surface area of the electrode was controlled by adhesive tape. A magnetic disc was placed on the back of the working electrode prior to the measurement.

Preparation of the magnetic beads modified with cortisol DNA aptamer

To modify streptavidin magnetic beads with CApt (method modified from streptavidin magnetic beads based on the description and protocol of New England Biolabs), various amounts of MBs (100, 200, 300, 400, and 500 μg) were washed with 100 μL wash/binding buffer for the pretreatment. A neodymium magnet was placed to the side of the tube, and the supernatant was removed. Then, 50 μL of different concentrations of CApt (0.1, 1.0, 2.0, 4.0, 6.0, 8.0, and 10 mg/mL) in the wash/binding buffer was added to prepare the streptavidin magnetic beads with CApt. The mixture was incubated at room temperature for 1 h under gentle rotation. Magnetic beads modified by CApt (CApt-MBs) were collected using the neodymium magnet, and the supernatant was removed. CApt-MBs were washed twice by adding 100 μL of wash/binding buffer. For each washing step, magnetic beads were re-suspended, the magnet was applied, and the supernatant was removed. Finally, prepared CApt-MBs were re-suspended in a low-salt buffer (0.15 mM NaCl, 20 mM Tris-HCl, and 1 mM EDTA; pH 7.5) and then were stored at 4 °C before use.

Immunoassay protocol

The prepared CApt-MBs suspension was transferred to a 1.5-mL microcentrifuge tube. The neodymium magnet was placed to the side of the tube, and the low-salt buffer supernatant was removed. CApt-MBs were incubated with different concentrations of cortisol (0.1, 0.5, 1, 5, 10, 50, and 100 ng/mL) at room temperature for 1 h. After the incubation, the supernatant was removed and CApt-MBs were washed with the wash/binding buffer. Next, CApt-MBs bound with cortisol were re-suspended in the low-salt buffer.

Electrochemical measurement

Electrochemical impedance spectrometry (EIS) and cyclic voltammetry (CV) were performed on an Autolab PGSTAT302N Potentiostat (Metrohm Siam Company Ltd., Switzerland) with impedance module FRA32M and controlled with the Nova 2.1.4 software. EIS measurement was performed in the frequency range of 100 kHz–0.01 Hz with a signal amplitude of 10 mV (vs Ag/AgCl). CV was performed from − 1.0 to 1.0 V (vs Ag/AgCl) with a scan rate of 0.1 V/s. All measurements were performed using 5 mM $[Fe(CN)_6]^{3-/4-}$ in 0.1 M KNO_3 as a redox solution at room temperature (25 ± 2 °C), and we obtained a Nyquist plot after 1 min of sample introduction (5 μL). The electrode design, schematic illustration at four different stages of the aptamer-based biosensor, and detection mechanism are shown in Fig. 1.

To determine cortisol, artificial human sweat with different concentrations of spiked cortisol was incubated with CApt-MBs at room temperature for 1 h using the aforementioned method. The electrochemical measurement was performed using freshly prepared CApt-MBs bound with cortisol. The recoveries of the spiked cortisol concentration were investigated. In addition, Zeta potential of CApt and CApt after binding with cortisol was investigated by Zetasizer Nano ZS (Malvern Panalytical, UK) to confirm the electrochemical behavior.

Results and discussion

Electrochemical characterization of aptamer-based biosensor

To characterize the aptamer-based biosensor, EIS and CV were employed to verify the electrode modification as shown in Fig. 2. For the EIS measurement, the impedance spectra (presented in the form of a Nyquist plot) were observed two parts: semi-circle and linear section. The semi-circle represents the electron-transfer process at high frequency, while the small linear section denotes the diffusion process at lower frequency. R_{ct} derived from the semi-circle diameter of the Nyquist plot indicates the electron transfer kinetic control of redox species at the electrode surface [35]. Figure 2 shows the Nyquist plots of the stepwise electrode modification in 5 mM $[Fe(CN)_6]^{3-/4-}$, which was fitted to the model of circuit (inset Fig. 2). The smallest semi-circle with R_{ct} of 5.89 ± 0.45 kΩ is observed from bare SPGE. When streptavidin MBs were introduced onto SPGE (MBs/SPGE), R_{ct} increases to 7.84 ± 0.53 kΩ, which indicates that a mass-transfer blocking barrier for $[Fe(CN)_6]^{3-/4-}$ towards the electrode surface occurred. Then, CApt-MBs were immobilized onto SPGE (CApt-MBs/SPGE), which results in the largest R_{ct} value (12.2 ± 0.05 kΩ) due to the electrostatic repulsion between negative charge of the DNA aptamer and $[Fe(CN)_6]^{3-/4-}$ redox solution [21, 36]. After cortisol was introduced onto the CApt-MB-modified electrode (cortisol/CApt-MBs/SPGE), R_{ct} decreases (11.6 ± 0.06 kΩ), which indicates the higher electron transfer to the electrode. We believe that the binding of cortisol and DNA aptamer should reduce the electrostatic repulsion, since the negative charge on the DNA aptamer was partially available [36]. Therefore, $[Fe(CN)_6]^{3-/4-}$ can easily transfer to the electrode surface. A consistent result as shown in Fig. S2 was achieved from CV compared with EIS. To confirm the

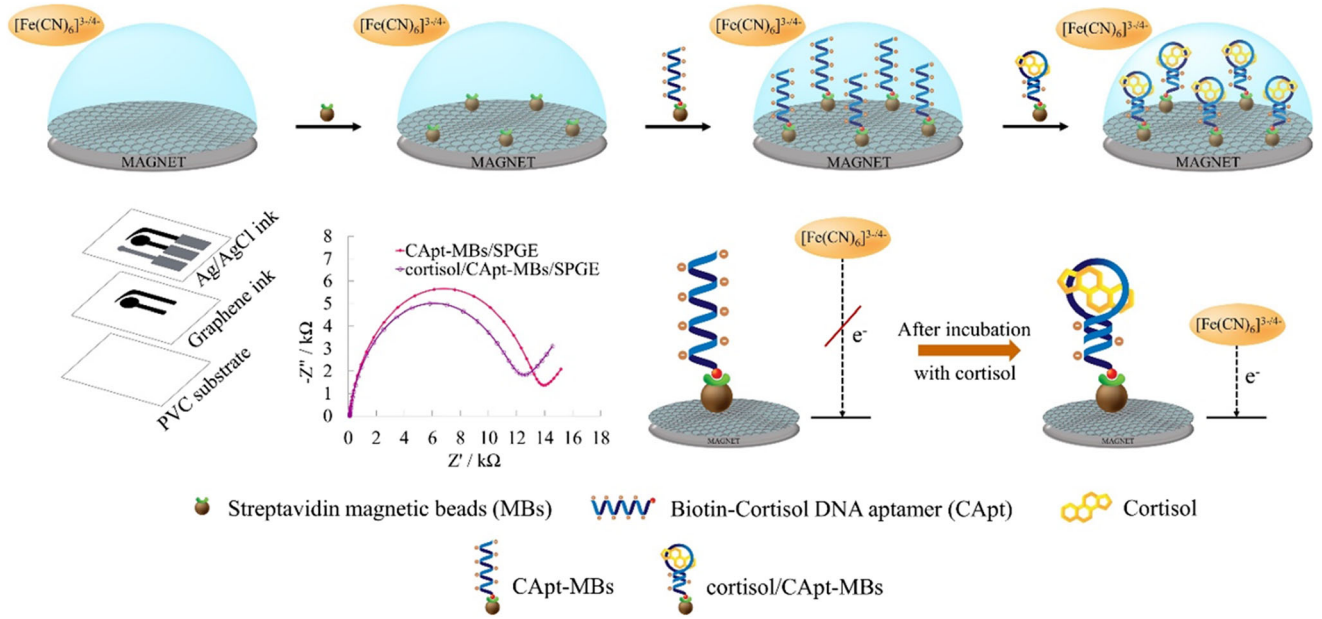

Fig. 1 Schematic illustration at four different stages of the aptamer-based biosensor and detection mechanism

electrochemical behavior, cortisol/CApt-MBs/SPGE was also evaluated using $[Ru(NH_3)_6^{2+/3+}]$ as the redox probe (Fig. S3). In addition, zeta potential of CApt and CApt after binding with cortisol was − 8.55 ± 0.45 mV and − 0.70 ± 0.04 mV, respectively. These results indicate that the negative charge on DNA aptamer decreases which corresponds to EIS and CV results.

Optimization of experimental variables

Amount of MBs

In terms of amount of MBs, the concentration of magnetic beads significantly affects the experimental results.

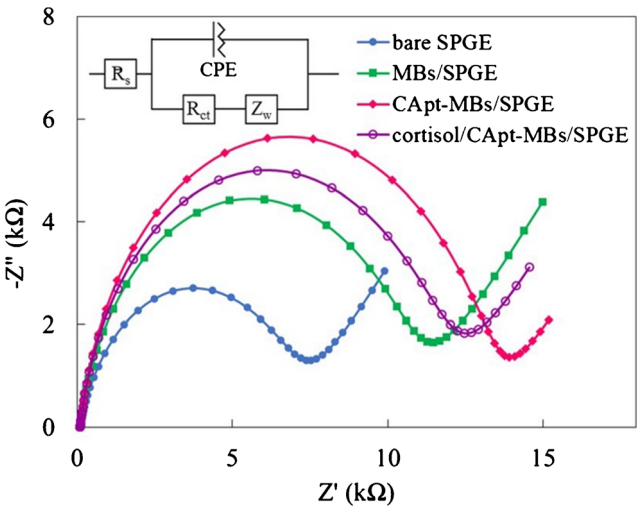

Fig. 2 Nyquist plots of: bare SPGE, MBs/SPGE, CApt-MBs/SPGE, and cortisol/CApt-MBs/SPGE

Excessive magnetic beads will cause waste, whereas insufficient magnetic beads significantly affect the sensitivity of the biosensors [37]. Various amounts of MBs (100, 200, 300, 400, and 500 μg) were studied (Fig. S4a). R_{ct} slightly increases with the increase in amount of MBs and tends to be stable at 300 μg of MBs. The low amount of MBs can increase the density aptamer packing, while an excess amount of MBs will increase aggregations. The aggregations can decrease the surface for DNA aptamer packing on MBs, which results in a constant R_{ct} [38]. As a result, 300 μg of MBs was selected as a suitable concentration for the CApt-MB fabrication.

CApt concentration

The effect of the CApt concentration on R_{ct} obtained from EIS was optimized as shown in Fig. S4b. Higher aptamer concentrations can provide more available active sites for the recognition of cortisol and affect the sensitivity [39]. R_{ct} increases with increasing CApt concentration and decreases to a plateau with CApt concentration above 2 mg/mL. This CApt concentration above 2 mg/mL will increase the steric hindrance or electrostatic repulsion of negative change between DNA aptamers, which decreases the density aptamer packing on MBs [40]. Therefore, 2 mg/mL of CApt concentration was selected as an optimal condition for all further experiments.

Incubation time

The incubation time is a crucial factor that can affect the analytical performance of the cortisol aptamer-based immunoassay. If there is insufficient time, the target cannot fully bind to the probe. If there is excess time, the non-specific adsorption

of the probe to the magnetic beads may be aggravated and interfere with the results [41]. The effect of the incubation time on 10 ng/mL of cortisol immobilized onto CApt-MBs was investigated at 30, 45, 60, 75, 90, and 120 min at room temperature, as shown in Fig. S4c. To evaluate the aptamer-based biosensor response, we considered the R_{ct} value of the aptamer-based biosensor after binding to cortisol. R_{ct} tended to be stable at 60 min of incubation. The likely reason is that the CApt-MBs were saturated by cortisol. In addition, the increase in incubation time provided higher binding efficiency between CApt-MBs and cortisol, which decreased R_{ct}. Moreover, a short incubation time was required for short-time analysis. In the following study, 60 min was selected as the optimal incubation time for cortisol-aptamer binding.

Analytical performance

The impedance spectra and calibration curve for the electrochemical determination of cortisol using the aptamer-based biosensor under optimal conditions were investigated. Figure 3a shows the EIS spectra for cortisol concentrations of 0.10–100 ng/mL. R_{ct} decreases with the increase in cortisol concentration. The inset in Fig. 2b shows that ΔR_{ct} has a good linear correlation with the logarithm of the cortisol concentration. The linear equation is presented as $\Delta R_{ct} = 466.86 \log C_{cortisol}$ (pg/mL) - 854.65 with a correlation coefficient (R^2) of 0.9939. The error bars represent the standard deviation of five measurements. The limit of detection (LOD) and limit of quantification (LOQ) were calculated to be 2.1 pg/mL and 12.7 pg/mL based on 3SD/slope and 10SD/slope, respectively. The analytical performance of the prepared aptamer-based biosensor for cortisol detection was also compared with previous reports (Table 1). Although the aptamer-based biosensor provides a narrower linear dynamic range than the other methods, this proposed aptamer-based biosensor is label-free, easy to fabricate, inexpensive, and disposable for cortisol detection. Compared with LOD presented by Dhull et al. 2019 [9], this proposed label-free biosensor has a higher LOD; however, it requires a complicated modification and multiple immobilization steps, and it needs to use antibodies as a biorecognition system.

Reproducibility, selectivity, and stability of the aptamer-based biosensor

To evaluate the reproducibility of the aptamer-based biosensor, five electrodes were investigated with different concentrations of cortisol: 1, 10, and 100 ng/mL. After measuring the electrochemical signal, we obtained the relative standard deviation (RSD) values of 0.55–1.65% (n = 5) (Fig. S5). This result demonstrates that the aptamer-based biosensor provided good reproducibility for cortisol detection.

In terms of selectivity, aptamer-based biosensors were investigated with two structurally similar steroids and three possible interferences in sweat. Cortisone, corticosterone, lactic acid, urea, and acetic acid were prepared at concentrations of 100 ng/mL and incubated with CApt-MBs/SPGE, which was followed by the R_{ct} measurement. The percent relative responses ($\%\Delta R_{ct}$) were evaluated from $((R_0 - R_{ct,in})/R_0) \times 100$, where R_0 and $R_{ct,in}$ are R_{ct} obtained before and after incubation in various species, respectively. As shown in Fig. 3c, the relative responses of other interferences were less than 5% compared with cortisol. However, the interference concentration was 10 times over that of cortisol. Thus, the aptamer-based biosensor offers good selectivity for the determination of cortisol.

The long-term stability of the prepared CApt-MBs/SPGE was estimated. CApt-MBs were prepared and subsequently stored at 4 °C. As shown in Fig. 3d, R_{ct} remained within ± 3SD (99.69 ± 0.59%) of its initial value for more than 30 days, which indicates a high stability of the cortisol aptamer-modified MBs. Therefore, CApt-MBs can be prepared and stored for further incubation with the cortisol solution.

Table 1 Analytical performance of the aptamer-based biosensor from the proposed method in comparison with previous methods

Substrate	Probe	Detection method	Limit of detection (pg/mL)	Linear range (pg/mL)	Labelling approach	Ref.
Graphene modified GCE	Pre-bound TA-Aptamer-AuNPs	Square wave voltammetry (SWV)	10	30–10^7	Labelling	[7]
MWCNT-Cu-porphyrin	MBs-Aptamer	Differential pulse voltammetry (DPV)	3.6	36–72 × 10^3	Label-free	[20]
MoS_2 nanosheet on flexible nanoporous membrane	Antibody	EIS	1 × 10^3	1 × 10^3–5 × 10^5	Label-free	[5]
AuNPs	Aptamer	Lateral flow assay (LFA)	1 × 10^3	1 × 10^3–3 × 10^5	Label-free	[10]
Nanostructure NiO thin film	Antibody	DPV	0.32	1–10^7	Label-free	[9]
Cy3 conjugated antibody	Antibody	Fluorescence-LFA	1 × 10^2	1 × 10^2–5 × 10^3	Labelling	[42]
SPGE	MBs-aptamer	EIS	2.14	1 × 10^2–1 × 10^5	Label-free	This work

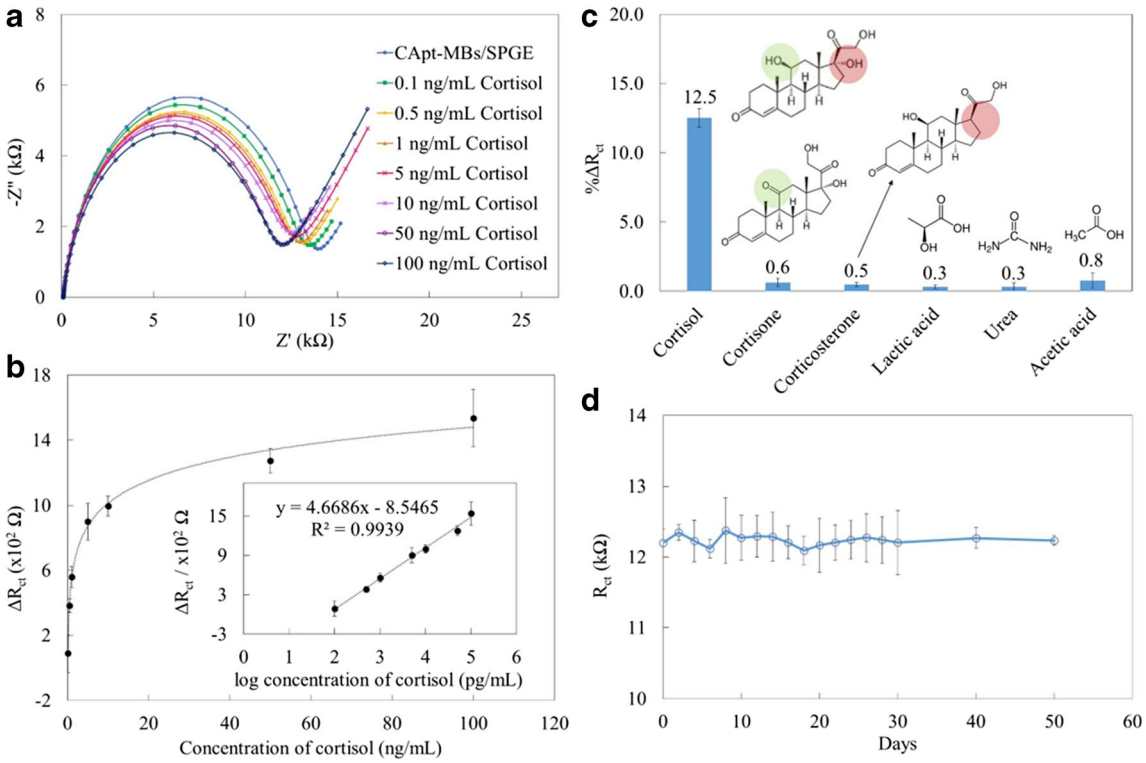

Fig. 3 **a** Nyquist plot measurements in 5 mM $[Fe(CN)_6]^{3-/4-}$ of the aptamer-based biosensor in different concentrations of cortisol (0, 0.1, 0.5, 1, 5, 10, 50, and 100 ng/mL). **b** Relationship between ΔR_{ct} and the concentrations of cortisol (inset is the calibration curve for cortisol determination). **c** Selectivity of the aptamer-based biosensor towards cortisone, corticosterone, lactic acid, urea, and acetic acid. **d** Stability of the prepared CApt-MBs for storage at 4 °C

Determination of cortisol in artificial human sweat

To demonstrate the applicability of the proposed system, the aptamer-based biosensor was applied to detect cortisol in artificial human sweat. Recovery testing was performed by the standard addition of artificial human sweat that contained different cortisol concentrations. Four concentration levels were spiked into artificial human sweat, and the final concentrations were 5, 20, 50, and 100 ng/mL, respectively. According to Table 2, the percent recoveries for cortisol were 97.4–109.2 with %RSD of 5.7–6.6. These results demonstrate that the aptamer-based biosensor can be used for cortisol detection in artificial human sweat with acceptable results.

Table 2 Determination of cortisol in artificial human sweat by the aptamer-based biosensor ($n = 5$)

Sample	Added (ng/mL)	Found (ng/mL) ± SD	%Recovery	%RSD
1	5	5.5 ± 0.4	109.2	6.6
2	20	19.5 ± 1.1	97.4	5.9
3	50	51.0 ± 2.9	101.9	5.7
4	100	106.8 ± 6.8	106.8	6.4

However, the aptamer-based biosensor provides potential limitation. This proposed method cannot directly introduce the sample onto the electrode surface to achieve cortisol binding with CApt-MBs. The incubation between CApt-MBs and cortisol in a microcentrifuge tube has been required.

Conclusions

An electrochemical impedance-based biosensor using a DNA aptamer (Apt) as a specific mode of molecular recognition was successfully developed to non-invasively detect cortisol. By relying on the label-free assay, cortisol was quantified by measuring ΔR_{ct} using EIS. A good linear relationship of the changes in charge-transfer resistance and logarithmic value of cortisol concentration with low detection limit was demonstrated. The aptamer-based biosensor demonstrated high sensitivity, reproducibility, selectivity, and long-term stability. Furthermore, the proposed system was successfully applied to quantify the cortisol level in artificial human sweat. As a result, the introduced approach can be an attractive substitute as a non-invasive and disposable sensing device with a facile fabrication process to monitor cortisol.

Supplementary Information The online version contains supplementary material available at https://doi.org/10.1007/s00604-020-04692-y.

Funding The authors thank financial supports from the Science Achievement Scholarship of Thailand (SAST), the 90th Anniversary of Chulalongkorn University Fund (Ratchadaphiseksompot Endowment Fund) (GCUGR1125633049D), National Research Council of Thailand (NRCT), and the Electrochemistry and Optical Spectroscopy Research Unit (EOSCE), Chulalongkorn University. PT would like to acknowledge the Second Century Fund (C2F), Chulalongkorn University, for providing the fellowship.

Compliance with ethical standards

Conflict of interest We have used artificial human sweat as analyte-free sample. Therefore, the human research ethics for the analysis of real sample are not required.

References

1. Fu HJ, Yuan LP, Shen YD, Liu YX, Liu B, Zhang SW, Xie ZX, Lei HT, Sun YM, Xu ZL (2018) A full-automated magnetic particle-based chemiluminescence immunoassay for rapid detection of cortisol in milk. Anal Chim Acta 1035:129–135. https://doi.org/10.1016/j.aca.2018.06.015
2. Kamarainen S, Maki M, Tolonen T, Palleschi G, Virtanen V, Micheli L, Sesay AM (2018) Disposable electrochemical immunosensor for cortisol determination in human saliva. Talanta 188:50–57. https://doi.org/10.1016/j.talanta.2018.05.039
3. Jeong G, Oh J, Jang J (2019) Fabrication of N-doped multidimensional carbon nanofibers for high-performance cortisol biosensors. Biosens Bioelectron 131:30–36. https://doi.org/10.1016/j.bios.2019.01.061
4. Kaushik A, Vasudev A, Arya SK, Pasha SK, Bhansali S (2014) Recent advances in cortisol sensing technologies for point-of-care application. Biosens Bioelectron 53:499–512. https://doi.org/10.1016/j.bios.2013.09.060
5. Kinnamon D, Ghanta R, Lin KC, Muthukumar S, Prasad S (2017) Portable biosensor for monitoring cortisol in low-volume perspired human sweat. Sci Rep 7(1):13312. https://doi.org/10.1038/s41598-017-13684-7
6. Jeon J, Uthaman S, Lee J, Hwang H, Kim G, Yoo PJ, Hammock BD, Kim CS, Park Y-S, Park I-K (2018) In-direct localized surface plasmon resonance (LSPR)-based nanosensors for highly sensitive and rapid detection of cortisol. Sensors Actuators B Chem 266:710–716. https://doi.org/10.1016/j.snb.2018.03.167
7. Sanghavi BJ, Moore JA, Chavez JL, Hagen JA, Kelley-Loughnane N, Chou CF, Swami NS (2016) Aptamer-functionalized nanoparticles for surface immobilization-free electrochemical detection of cortisol in a microfluidic device. Biosens Bioelectron 78:244–252. https://doi.org/10.1016/j.bios.2015.11.044
8. Li C, Zhang Z, Liu X, Shen K, Gu P, Kang X (2017) Simultaneous quantification of cortisol and cortisone in urines from infants with packed-fiber solid-phase extraction coupled to HPLC-MS/MS. J Chromatogr B Anal Technol Biomed Life Sci 1061-1062:163–168. https://doi.org/10.1016/j.jchromb.2017.07.012
9. Dhull N, Kaur G, Gupta V, Tomar M (2019) Highly sensitive and non-invasive electrochemical immunosensor for salivary cortisol detection. Sensors Actuators B Chem 293:281–288. https://doi.org/10.1016/j.snb.2019.05.020
10. Dalirirad S, Steckl AJ (2019) Aptamer-based lateral flow assay for point of care cortisol detection in sweat. Sensors Actuators B Chem 283:79–86. https://doi.org/10.1016/j.snb.2018.11.161
11. Bravo AM, Castro MDL (2014) Sweat: a sample with limited present applications and promising future in metabolomics. J Pharm Biomed Anal 90:139–147. https://doi.org/10.1016/j.jpba.2013.10.048
12. Heikenfeld J (2016) Non-invasive analyte access and sensing through eccrine sweat: challenges and outlook circa 2016. Electroanalysis 28(6):1242–1249. https://doi.org/10.1002/elan.201600018
13. Kobayashi N, Sun P, Fujimaki Y, Niwa T, Nishio T, Goto J, Hosoda H (2002) Generation of a novel monoclonal antibody against cortisol[C-4]-bovine serum albumin conjugate: Application to enzyme-linked immunosorbent assay for urinary and serum cortisol. Anal Sci 18:1309–1314. https://doi.org/10.2116/analsci.18.1309
14. Ito T, Aoki N, Shinobu W, Suzuki K (2014) Duplicate analysis of cortisol for stress check using QCM with a self–suction flow system. Procedia Eng. 87:296–299. https://doi.org/10.1016/j.proeng.2014.11.666
15. Yao Y, Jiang C, Ping J (2019) Flexible freestanding graphene paper-based potentiometric enzymatic aptasensor for ultrasensitive wireless detection of kanamycin. Biosens Bioelectron 123:178–184. https://doi.org/10.1016/j.bios.2018.08.048
16. Ma F, Yan J, Sun L, Chen Y (2019) Electrochemical impedance spectroscopy for quantization of matrix Metalloproteinase-14 based on peptides inhibiting its homodimerization and heterodimerization. Talanta 205:120142. https://doi.org/10.1016/j.talanta.2019.120142
17. He B, Dong X (2019) Hierarchically porous Zr-MOFs labelled methylene blue as signal tags for electrochemical patulin aptasensor based on ZnO nano flower. Sensors Actuators B Chem 294:192–198. https://doi.org/10.1016/j.snb.2019.05.045
18. Jampasa S, Siangproh W, Laocharoensuk R, Vilaivan T, Chailapakul O (2018) Electrochemical detection of c-reactive protein based on anthraquinone-labeled antibody using a screen-printed graphene electrode. Talanta 183:311–319. https://doi.org/10.1016/j.talanta.2018.02.075
19. Makhneva E, Farka Z, Skládal P, Zajíčková L (2018) Cyclopropylamine plasma polymer surfaces for label-free SPR and QCM immunosensing of Salmonella. Sensors Actuators B Chem 276:447–455. https://doi.org/10.1016/j.snb.2018.08.055
20. Fernandez RE, Umasankar Y, Manickam P, Nickel JC, Iwasaki LR, Kawamoto BK, Todoki KC, Scott JM, Bhansali S (2017) Disposable aptamer-sensor aided by magnetic nanoparticle enrichment for detection of salivary cortisol variations in obstructive sleep apnea patients. Sci Rep 7(1):17992. https://doi.org/10.1038/s41598-017-17835-8
21. Teengam P, Siangproh W, Tuantranont A, Vilaivan T, Chailapakul O, Henry CS (2018) Electrochemical impedance-based DNA sensor using pyrrolidinyl peptide nucleic acids for tuberculosis detection. Anal Chim Acta 1044:102–109. https://doi.org/10.1016/j.aca.2018.07.045
22. Bai C, Lu Z, Jiang H, Yang Z, Liu X, Ding H, Li H, Dong J, Huang A, Fang T, Jiang Y, Zhu L, Lou X, Li S, Shao N (2018) Aptamer selection and application in multivalent binding-based electrical impedance detection of inactivated H1N1 virus. Biosens Bioelectron 110:162–167. https://doi.org/10.1016/j.bios.2018.03.047
23. Liang G, Man Y, Jin X, Pan L, Liu X (2016) Aptamer-based biosensor for label-free detection of ethanolamine by electrochemical impedance spectroscopy. Anal Chim Acta 936:222–228. https://doi.org/10.1016/j.aca.2016.06.056
24. Gao S, Hu W, Zheng X, Cai S, Wu J (2019) Functionalized aptamer with an antiparallel G-quadruplex: Structural remodeling,

recognition mechanism, and diagnostic applications targeting CTGF. Biosens Bioelectron 142:111475. https://doi.org/10.1016/j.bios.2019.111475
25. Weng X, Neethirajan S (2017) Aptamer-based fluorometric determination of norovirus using a paper-based microfluidic device. Microchim Acta 184(11):4545–4552. https://doi.org/10.1007/s00604-017-2467-x
26. Kiruba Daniel SCG, Kumar A, Sivasakthi K, Thakur CS (2019) Handheld, low-cost electronic device for rapid, real-time fluorescence-based detection of Hg2+, using aptamer-templated ZnO quantum dots. Sensors Actuators B Chem 290:73–78. https://doi.org/10.1016/j.snb.2019.03.113
27. Luo Y, Wang J, Yang L, Gao T, Pei R (2018) In vitro selection of DNA aptamers for the development of fluorescent aptasensor for sarcosine detection. Sensors Actuators B Chem 276:128–135. https://doi.org/10.1016/j.snb.2018.08.105
28. Abnousa K, Daneshc NM, R M, Alibolandia M, Taghdisi SM (2018) A novel electrochemical sensor for bisphenol A detection based on nontarget-induced extension of aptamer length and formation of a physical barrier. Biosens Bioelectron 119:204–208. https://doi.org/10.1016/j.bios.2018.08.024
29. Feng S, Chen C, Wang W, Que L (2018) An aptamer nanopore-enabled microsensor for detection of theophylline. Biosens Bioelectron 105:36–41. https://doi.org/10.1016/j.bios.2018.01.016
30. Zhou L, Wang M-H, Wang J-P, Ye Z-Z (2011) Application of biosensor surface immobilization methods for aptamer. Chin J Anal Chem 39(3):432–438. https://doi.org/10.1016/s1872-2040(10)60429-x
31. Balamurugan S, Obubuafo A, Soper SA, Spivak DA (2008) Surface immobilization methods for aptamer diagnostic applications. Anal Bioanal Chem 390(4):1009–1021. https://doi.org/10.1007/s00216-007-1587-2
32. Xue Y, Jiang D-l, Hu Q, Rao S-q, Gao L, Yang Z-q (2019) Electrochemical magnetic bead-based immunosensor for rapid and quantitative detection of probiotic Lactobacillus rhamnosus in dairy products. Food Anal Methods 12(5):1197–1207. https://doi.org/10.1007/s12161-019-01457-z
33. Modh H, Scheper T, Walter JG (2018) Aptamer-modified magnetic beads in biosensing. Sensors (Basel) 18(4). https://doi.org/10.3390/s18041041
34. Teengam P, Siangproh W, Tuantranont A, Henry CS, Vilaivan T, Chailapakul O (2017) Electrochemical paper-based peptide nucleic acid biosensor for detecting human papillomavirus. Anal Chim Acta 952:32–40. https://doi.org/10.1016/j.aca.2016.11.071
35. Randviir EP, Banks CE (2013) Electrochemical impedance spectroscopy: an overview of bioanalytical applications. Anal Methods 5(5):1098. https://doi.org/10.1039/c3ay26476a
36. Ghanbari K, Roushani M (2018) A nanohybrid probe based on double recognition of an aptamer MIP grafted onto a MWCNTs-Chit nanocomposite for sensing hepatitis C virus core antigen. Sensors Actuators B Chem 258:1066–1071. https://doi.org/10.1016/j.snb.2017.11.145
37. Mao K, Yang Z, Li J, Zhou X, Li X, Hu J (2017) A novel colorimetric biosensor based on non-aggregated Au@Ag core-shell nanoparticles for methamphetamine and cocaine detection. Talanta 175:338–346. https://doi.org/10.1016/j.talanta.2017.07.011
38. Erdem A, Pividori MI, Lermo A, Bonanni A, del Valle M, Alegret S (2006) Genomagnetic assay based on label-free electrochemical detection using magneto-composite electrodes. Sensors Actuators B Chem 114(2):591–598. https://doi.org/10.1016/j.snb.2005.05.031
39. Ocana C, Hayat A, Mishra RK, Vasilescu A, Del Valle M, Marty JL (2015) Label free aptasensor for Lysozyme detection: a comparison of the analytical performance of two aptamers. Bioelectrochemistry 105:72–77. https://doi.org/10.1016/j.bioelechem.2015.05.009
40. Liu Y, Tuleouva N, Ramanculov E, Revzin A (2010) Aptamer-based electrochemical biosensor for interferon gamma detection. Anal Chem 82(19):8131–8136. https://doi.org/10.1021/ac101409t
41. Yu X, He L, Pentok M, Yang H, Yang Y, Li Z, He N, Deng Y, Li S, Liu T, Chen X, Luo H (2019) An aptamer-based new method for competitive fluorescence detection of exosomes. Nanoscale 11(33):15589–15595. https://doi.org/10.1039/c9nr04050a
42. Shin J, Kim S, Yoon T, Joo C, Jung HI (2019) Smart fatigue phone: real-time estimation of driver fatigue using smartphone-based cortisol detection. Biosens Bioelectron 136:106–111. https://doi.org/10.1016/j.bios.2019.04.046